

Supplementary Information

Zika virus-encoded NS2A disrupts mammalian cortical neurogenesis by degrading adherens junction proteins

Ki-Jun Yoon, Guang Song, Xuyu Qian, Jianbo Pan, Dan Xu, Hee Sool Rho, Nam-Shik Kim, Christa Habela, Lily Zheng, Fadi Jacob, Feiran Zhang, Emily M. Lee, Wei-Kai Huang, Francisca Rojas Ringeling, Caroline Vissers, Cui Li, Ling Yuan, Koeun Kang, Sunghan Kim, Junghoon Yeo, Yichen Cheng, Sheng Liu, Zhexing Wen, Cheng-Feng Qin, Qingfeng Wu, Kimberly M. Christian, Hengli Tang, Peng Jin, Zhiheng Xu, Jiang Qian, Heng Zhu, Hongjun Song and Guo-li Ming

Inventory

Figures S1-6

Tables S1-4

Supplementary Figures

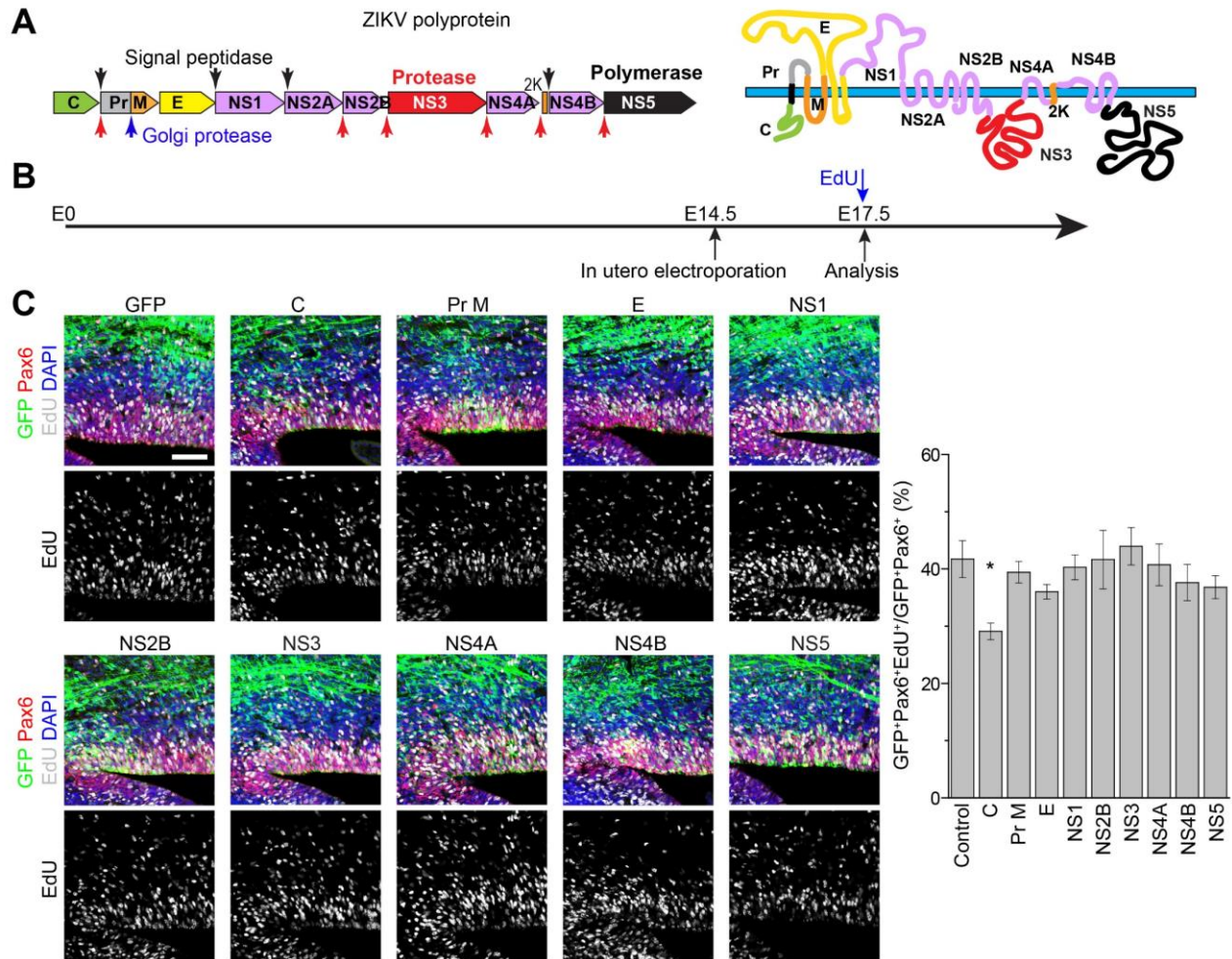


Figure S1. Screen of individual ZIKV encoded proteins for regulation of mouse embryonic cortical radial glial cell proliferation in vivo, related to Figure 1.

(A) A schematic diagram of the ZIKV polyprotein (left panel) and topological arrangement of individual viral proteins on the endoplasmic reticulum membrane (right panel).

(B) A schematic diagram of the procedure for in utero electroporation and analysis.

(C) Sample confocal images of immunostaining for Pax6, GFP, and staining for EdU and DAPI (left panels; scale bar: 100 μ m) and quantification (right panel) under different conditions. Embryonic mouse cortex was electroporated at E14.5 to express GFP, or GFP plus one ZIKV encoded protein, followed by EdU labeling 2 hr before analysis at E17.5. Values represent mean \pm SEM ($n = 4-5$ animals; * $P < 0.05$; Student's t-test).

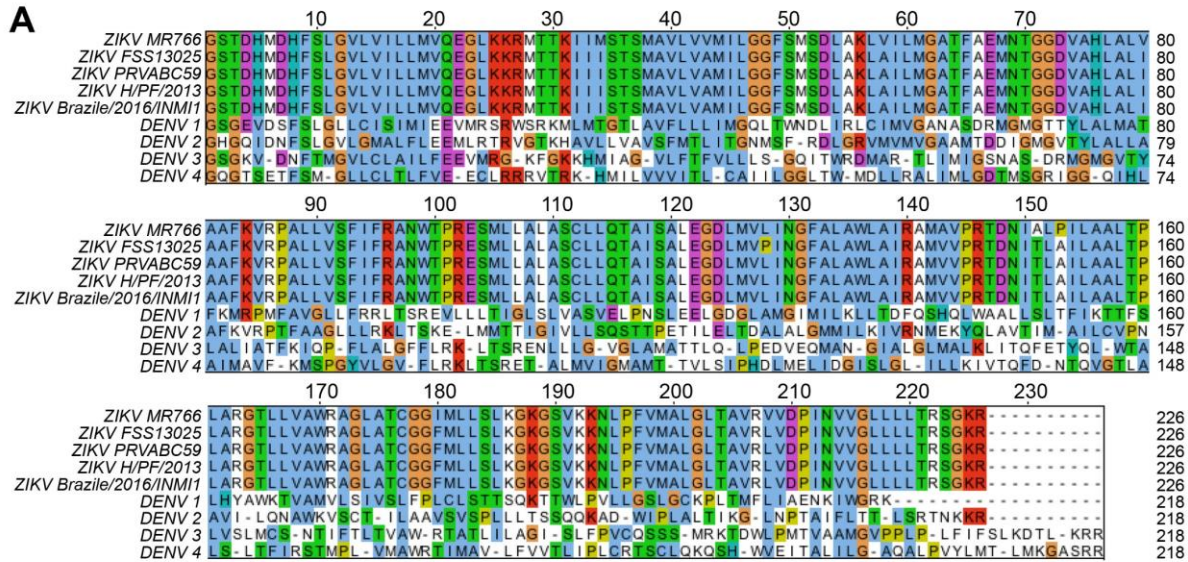


Figure S2. Homology of NS2A proteins among different ZIKV and DENV strains, related to Figure 1.

(A) Alignment of NS2A proteins from different ZIKV and DENV strains. ZIKV MR766: African origin; 2016/INMI1: Brazilian origin; PRVABC59: Puerto Rican origin; FSS13025: Cambodian origin; H/PF/2013: French Polynesian; DENV1-4: Dengue Virus Serotype 1-4.

(B) Quantification of differences at the protein coding level among NS2A proteins from different ZIKV and DENV strains, calculated by average distance using % identity of amino acids.

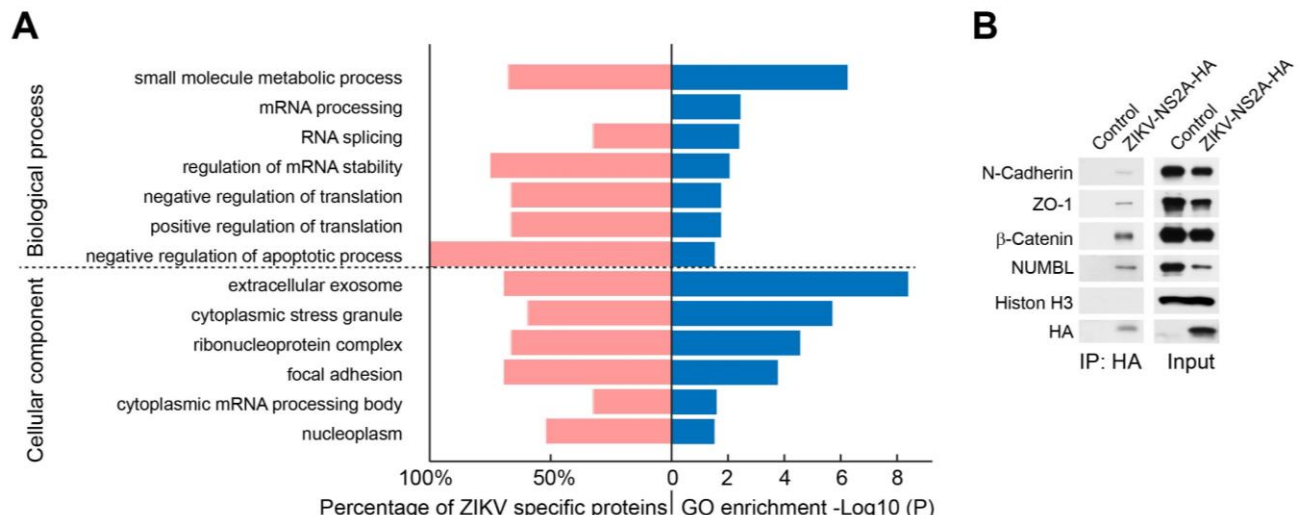


Figure S3. GO analysis of protein-protein interactomes and validation of some interactions in mouse neural progenitors, related to Figure 3.

(A) GO analysis of ZIKV-NS2A and DENV-NS2A interacting proteins for biological processes and cellular components. Quantifications of ZIKV-NS2A specific interacting proteins in these GO terms are also shown.

(B) Co-IP analysis of ZIKV-NS2A-HA with adherens junction complex components upon transfection of ZIKV-NS2A-HA into mouse cortical neural progenitors.

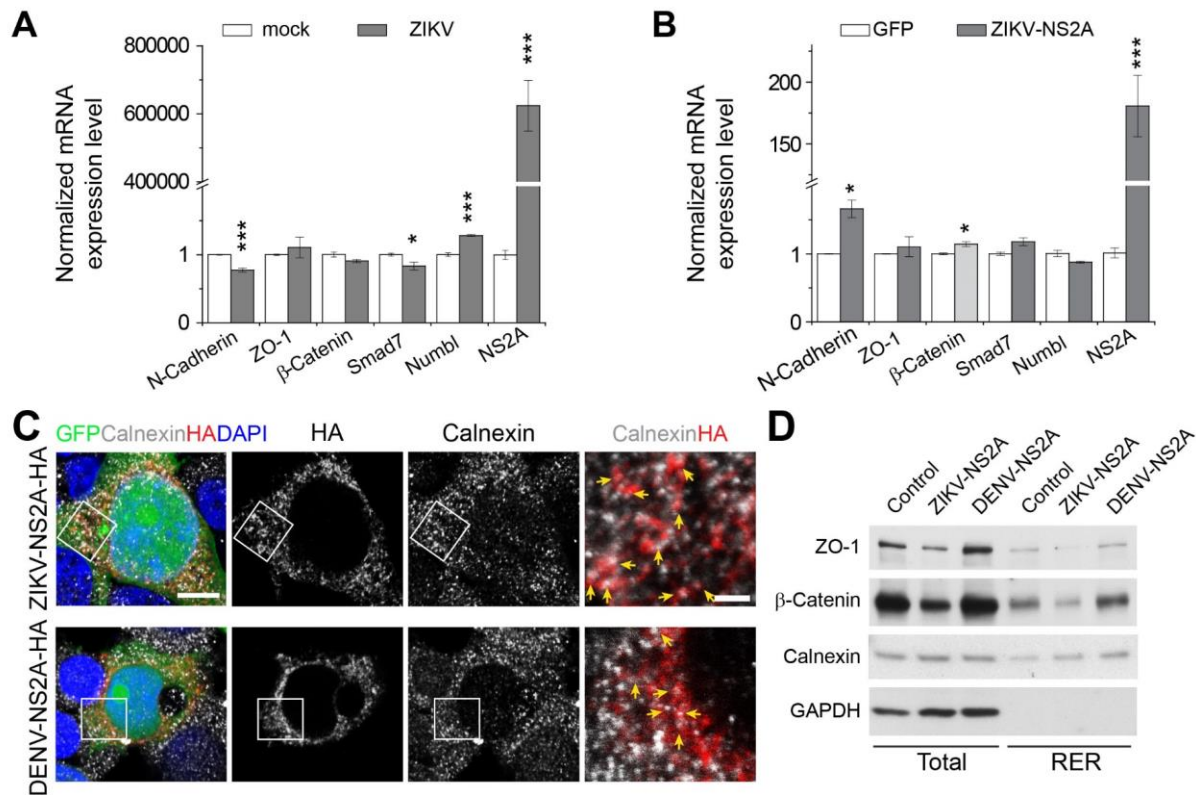


Figure S4. Quantification of mRNA levels for adherens junction complex components and endoplasmic reticulum (ER) localization of ZIKV-NS2A and DENV-NS2A proteins, related to Figure 4.

(A-B) Quantification of mRNA levels for adherens junction complex components upon ZIKV infection (A), or ZIKV-NS2A expression (B), in mouse neural progenitor cells by Q-PCR. Data were normalized to that of mock treatment for ZIKV infection (A), or to that of GFP alone for ZIKV-NS2A (B). Values represent mean \pm SEM (n = 4 experiments; *** P < 0.001; * P < 0.05; One-way ANOVA). (C) Sample images of immunostaining of HA-tagged NS2A, Calnexin, an ER marker, and staining for DAPI (left panels; scale bar: 10 μ m). Magnified images are also shown (right panel; scale bar: 2 μ m). Arrows point to co-localized puncta.

(D) Reduced levels of adherens junction complex components with ER compartments upon expression of ZIKV-NS2A, but not DENV-NS2A. Sample western blot images of total cell lysates and the rough ER fractionation (RER) are shown.

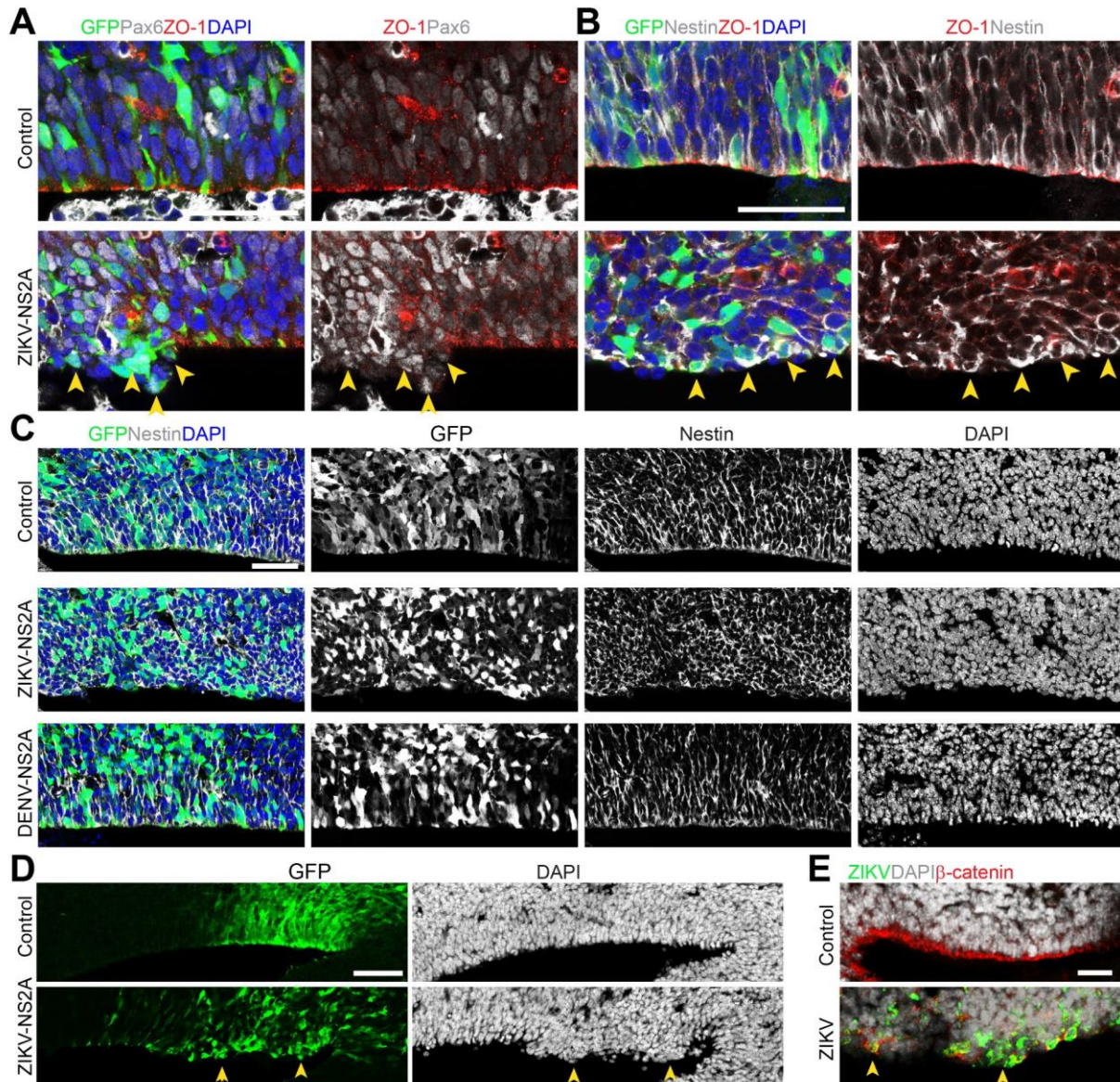


Figure S5. Disruption of radial glial organization in the embryonic mouse cortex in vivo upon expression of ZIKV-NS2A or ZIKV infection, but not DENV-NS2A, related to Figure 5.

(A-D) Embryonic mouse cortex was electroporated at E14.5 to express GFP, GFP and ZIKV-NS2A, or GFP and DENV-NS2A, and analyzed at E17.5. In (A, B), sample images of immunostaining for Pax6, ZO-1, Nestin and GFP, and staining for DAPI are shown. Scale bars: 50 μ m. Note the expression of ZO-1 in Pax6⁺ or Nestin⁺ radial glial cells expressing GFP, but not those co-expressing GFP and ZIKV-NS2A (highlighted by arrows). In (C), sample images of immunostaining for Nestin, GFP and staining for DAPI are shown. Scale bar: 50 μ m. Note disorganized radial fibers upon ZIKV-NS2A expression. In (D), sample images of GFP immunostaining and DAPI staining are shown. Scale bar: 50 μ m. Arrows point to regions with ventricular protrusions.

(E) ZIKV-SZ strain or PBS was injected into the lateral ventricles of E13.5 ICR mice and examined at P3. Sample images of immunostaining for ZIKV and β -catenin and DAPI are shown. Scale bar: 25 μ m. Arrows point to regions with ventricular protrusions.

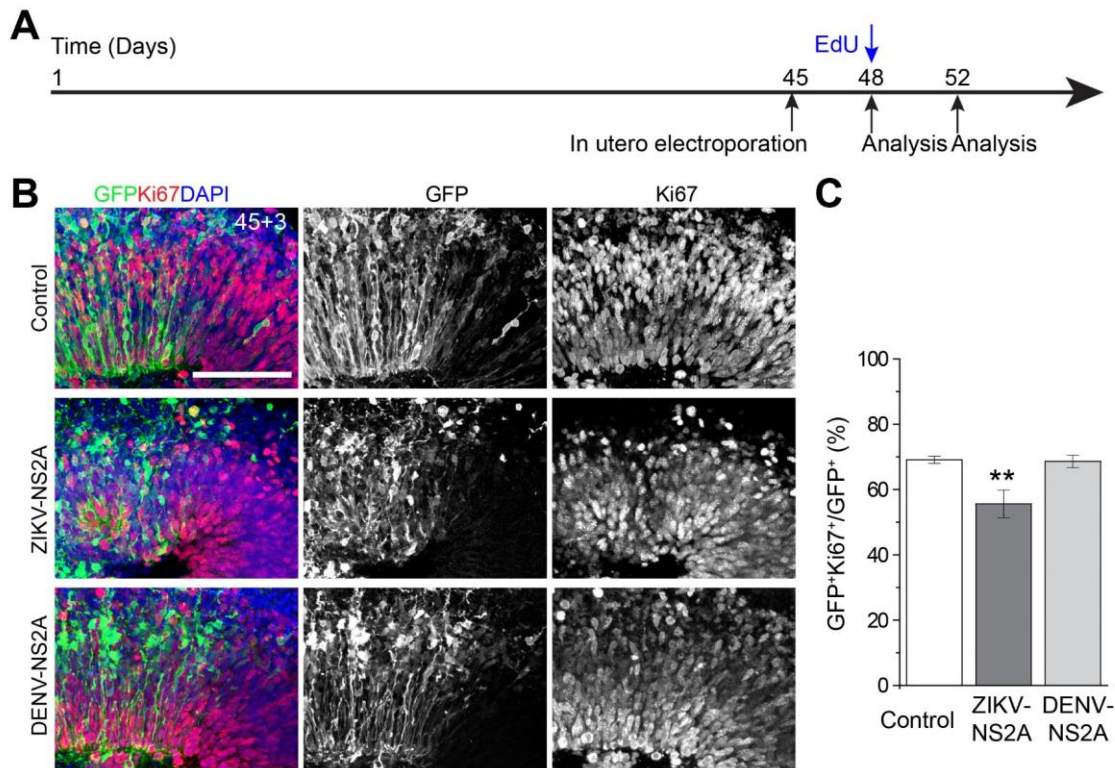


Figure S6. Expression of ZIKV-NS2A, but not DENV-NS2A, affects proliferation of ventricular RGCs in human forebrain organoids, related to Figure 6.

(A) A schematic diagram of the experimental procedure.

(B) Sample images of immunostaining for cell proliferation marker Ki67, GFP, and staining for DAPI for samples at 45+3 days. Scale bar: 100 μ m. Note the disorganization of GFP⁺ radial fibers upon ZIKV-NS2A expression (middle panel).

(C) Quantification of proliferation at 45+3 days. Values represent mean \pm SEM (n = 10 organoids; ** $P < 0.01$; Student's t-test).

Supplementary Tables

Table S1. List of primers used to clone ORFs of ZIKV encoded proteins and primers used for Q-PCR analysis, related to STAR Methods. (See the Excel file).

Table S2. List of ZIKV-NS2A and DENV-NS2A interacting proteins across the human proteome, related to Figure 3. (See the Excel file).

Table S3. List of gene ontology enrichment terms for ZIKV-NS2A and DENV-NS2A binding proteins, related to Figure 3. (See the Excel file).

Table S4. List of ZIKV-NS2A interacting proteins within the functional protein association network, related to Figure 3. (See the Excel file).